Low Temperature Physics/Fizika Nizkikh Temperatur, 2014, v. 40, No. 4, pp. 484–491

Magnetic quantum oscillations in the charge-density-wave state of the organic metals α-(BEDT-TTF)$_2$MHg(SCN)$_4$ with M = K and Tl

M.V. Kartsovnik[1], V.N. Zverev[2,3], D. Andres[1*], W. Biberacher[1], T. Helm[1**], P.D. Grigoriev[4], R. Ramazashvili[5], N.D. Kushch[6], and H. Müller[7]

[1]*Walther-Meissner-Institut, Bayerische Akademie der Wissenschaften*
Walther-Meissner-Strasse 8, Garching D-85748, Germany
E-mail: mark.kartsovnik@wmi.badw.de

[2]*Institute of Solid State Physics, Russian Academy of Sciences*
Academician Ossipyan Str. 2, Chernogolovka 142432, Russia

[3] *Moscow Institute of Physics and Technology, Dolgoprudny, Institutskii per. 9, Moscow reg., 141700, Russia*

[4]*L.D. Landau Institute for Theoretical Physics, Russian Academy of Sciences*
Academician Semenov Ave. 1a, Chernogolovka 142432, Russia

[5]*Laboratoire de Physique Théorique – IRSAMC, CNRS and Université de Toulouse*
UPS, F-31062 Toulouse, France

[6]*Institute of Problems of Chemical Physics, Russian Academy of Sciences*
Academician Semenov Ave. 1, Chernogolovka 142432, Russia

[7]*European Synchrotron Radiation Facility, Rue Jules Horowitz 6, BP 220, 38043 Grenoble CEDEX 9, France*

Received November 23, 2013

The low-temperature charge-density-wave (CDW) state in the layered organic metals α-(BEDT-TTF)$_2$MHg(SCN)$_4$ has been studied by means of the Shubnikov–de Haas and de Haas–van Alphen effects. In addition to the dominant α-frequency, which is also observed in the normal state, both the magnetoresistance and magnetic torque possess a slowly oscillating component. These slow oscillations provide a firm evidence for the CDW-induced reconstruction of the original cylindrical Fermi surface. The α-oscillations of the interlayer magnetoresistance exhibit an anomalous phase inversion in the CDW state, whereas the de Haas–van Alphen signal maintains the normal phase. We argue that the anomaly may be attributed to the magnetic-breakdown origin of the α-oscillations in the CDW state. A theoretical model illustrating the possibility of a phase inversion in the oscillating interlayer conductivity in the presence of a spatially fluctuating magnetic breakdown gap is proposed.

PACS: 72.15.Gd Galvanomagnetic and other magnetotransport effects;
74.70.Kn Organic superconductors;
71.45.Lr Charge-density-wave systems.

Keywords: organic metals, Shubnikov–de Haas effect, de Haas–van Alphen effect, charge-density wave, magnetic breakdown.

* Present address: Attocube Systems AG, Königinstrasse 11a, München 80539, Germany.

** Present address: Material Science Devision, Lawrence Berkeley National Laboratory 62R0203, 1 Cyclotron Road, Berkeley 94720, CA, USA.

1. Introduction

Comprehensive quantitative description of the de Haas–van Alphen effect by the Lifshitz–Kosevich theory has made magnetic quantum oscillations (MQO) one of the most powerful tools for studying conduction electrons in metals. This tool has been extensively used not only for exploring conventional metals [1] but also for gaining a deep insight into electronic systems of more complex materials such as cuprate [2,3] and iron-based [4,5] high-temperature superconductors, heavy fermion compounds [6] and organic charge-transfer salts [7]. Particularly the latter class of materials has demonstrated the great potential of the de Haas–van Alphen (dHvA) and Shubnikov–de Haas (SdH) effects in revealing the Fermi-surface properties in various electronic states. Additionally, the organic compounds, generally characterized by an extraordinary crystal quality, very high anisotropy, and significant electron interactions, offer a vast playground for studying specific features of MQO in layered correlated electron systems, see for a review Refs. 7–10 and references therein.

A spectacular example of how MQO and high-field classical magnetoresistance can be used for investigating the electronic state of an organic metal is the work done on α-(BEDT-TTF)$_2$MHg(XCN)$_4$, where BEDT-TTF stands for the donor organic molecule bis(ethylenedithio)tetrathiafulvalene, M = K, Tl, NH_4, and Rb, and X = S, Se, see [7] for a review. These are isostructural layered charge-transfer salts with the Fermi surface comprising a pair of slightly warped open sheets (representing a quasi-one-dimensional, q1D, conduction band) and a cylinder (a quasi-two-dimensional, q2D, band) [11,12]. The compounds display a huge electronic anisotropy: the ratio of the effective transfer integrals within and across conducting layers $t_{\|}/t_{\perp}$ is in the range 10^2–10^3 [13,14]. As a result, the MQO have a very large amplitude and bear a pronounced 2D character [15–19]. The monotonic part of the interlayer magnetoresistance also shows severe deviations from the conventional three-dimensional behavior [14,19,20].

At temperature $T \sim 10$ K three salts, with M = K, Tl, and Rb, and X = S undergo a charge-density-wave (CDW) transition caused by the Peierls-type nesting instability of the open Fermi sheets [7,21]. The compounds remain, however, metallic due to the ungapped cylindrical Fermi surface. The low-temperature state is characterized by a bunch of striking anomalies in high magnetic fields which, actually, have triggered the initial interest in these materials [22–26]. By now, it is clear that their behavior is largely governed by the coexistence of a narrow-gap CDW and metallic q2D carriers and, consequently, a rich phase diagram including several kinds of magnetic field-induced transitions between different CDW states, see, e.g., [27–30]. However, a number of anomalies are still a matter of debate. One of the problems in this respect is that there is no general consensus as to the exact topology of the reconstructed Fermi surface in the CDW state [25,31–33]. Moreover, even the occurrence of reconstruction itself has been questioned [34,35].

Here we report on experimental studies of magnetic quantum oscillations in the CDW state of α-(BEDT-TTF)$_2$MHg(SCN)$_4$ with M = K and Tl. In addition to the dominant frequency corresponding to the large cylindrical Fermi surface predicted by the normal-state band structure calculations [11,12], a new, low frequency is found in both the SdH and dHvA spectra. This result is discussed in terms of the Fermi surface reconstruction in the CDW state. Further, the phase of the SdH (but not dHvA!) oscillations in the low-temperature, low-field CDW state is shown to be inverted in comparison to that in the normal state. We propose a model that qualitatively explains this anomalous behavior via spatial fluctuations of the magnetic breakdown gap.

2. Experimental

The experiments were carried out on α-(BEDT-TTF)$_2$KHg(SCN)$_4$ and α-(BEDT-TTF)$_2$TlHg(SCN)$_4$ single crystals hereafter referred to as the K- and Tl-salt, respectively. The samples were submillimeter-size platelets of a distorted hexagon shape with large faces parallel to the highly conducting BEDT-TTF layers. For ambient-pressure studies a setup allowing simultaneous measurements of the interlayer magnetoresistance and magnetic torque [36] was used. High-pressure magnetoresistance experiments were done using a small clamp pressure cell made of nonmagnetic Cu–Be alloy. The pressure was applied at room temperature and its low-T value was determined from the resistance of a calibrated manganin pressure gauge. The oscillations of magnetoresistance and magnetic torque were studied in the temperature range from 0.4 to 4.2 K. Magnetic fields up to 17 T were generated by a superconducting solenoid. Experiments at higher fields, up to 29 T, were conducted at the Laboratoire National des Champs Magnétiques Intenses (LNCMI), Grenoble, France.

3. MQO spectrum in the CDW$_0$ state

The magnetoresistance and magnetization of the α-(BEDT-TTF)$_2$MHg(SCN)$_4$ salts in the CDW state were studied by many authors, see [7] and references therein. The general behavior in a field nearly perpendicular to conducting BEDT-TTF layers is illustrated in Fig. 1. Below the so-called kink field, B_k = 24 and 27 T for the K- and Tl-salts, respectively [22,37], the zero-field CDW$_0$ state is stable. As seen from Fig. 1, it is characterized by a very high interlayer magnetoresistance showing a peak at around 10 T and then gradually turning down. The MQO in the CDW$_0$ state are moderately strong, of the order of a few percent of the total signal, and have a distorted or even split shape due to an anomalously strong second harmonic contribution. At B_k the system is driven into the CDW$_x$ state

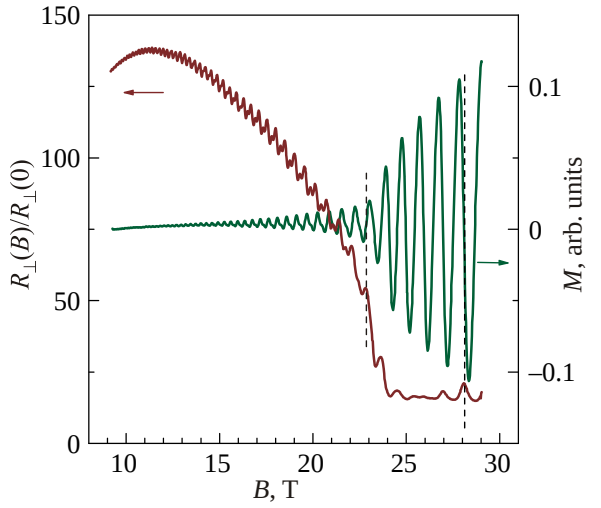

Fig. 1. (Color online) Field-dependent interlayer resistance (left-hand scale) and magnetization (derived from torque measurements, right-hand scale) of the K-salt in the CDW state; $T = 1.4$ K; the field is tilted by angle $\theta = 6.2°$ from the direction perpendicular to the conducting layers.

[38,39] with a B-dependent spatially modulated order parameter analogous to the Larkin–Ovchinnikov–Fulde–Ferrel state predicted for superconductors [40–42]. Both the dHvA and SdH oscillations are strongly enhanced upon entering this state: for example, the SdH amplitude in Fig. 1 amounts to ≈30% of the nonoscillating background at 28 T.

Figure 2 shows the oscillatory components of the interlayer magnetoresistance (a) and torque (b) of the K-salt in the CDW_0 state and (inset) their fast Fourier transform (FFT) spectra. In order to obtain an appreciable signal in the torque, the field is tilted by the angle $\theta = 31.5°$ from the normal to the layers. The oscillations are dominated by the fundamental frequency $F_\alpha = 787$ T. In agreement with earlier experiments, this frequency, recalculated to the purely out-of-plane field orientation, $F_{\alpha,0} = F_\alpha(\theta)\cos\theta = 670$ T, corresponds to the cylindrical Fermi surface with the same area as in the normal state, see Fig. 2(c).

In addition to F_α and its higher harmonics, a low-frequency peak at $F_\lambda = 210$ T is clearly pronounced in the FFT spectra. It is important that the low frequency is observed not only in magnetoresistance but also in magnetization. The latter establishes its thermodynamic origin, ruling out kinetic effects like quantum interference of open electron trajectories [43] or due to a weak warping of the Fermi cylinder [44] which are often found in layered organic metals [8,9]. We, therefore, attribute it to a real closed orbit on a small cylindrical Fermi surface undergoing Landau quantization in a strong magnetic field.

The present result provides a solid argument in favor of the Fermi surface reconstruction model based on studies of the semiclassical angle-dependent magnetoresistance oscillations (AMRO) [25]. According to this model, the CDW potential $V_{\mathbf{Q}}$ with the wave vector $\mathbf{Q}$, besides nesting the

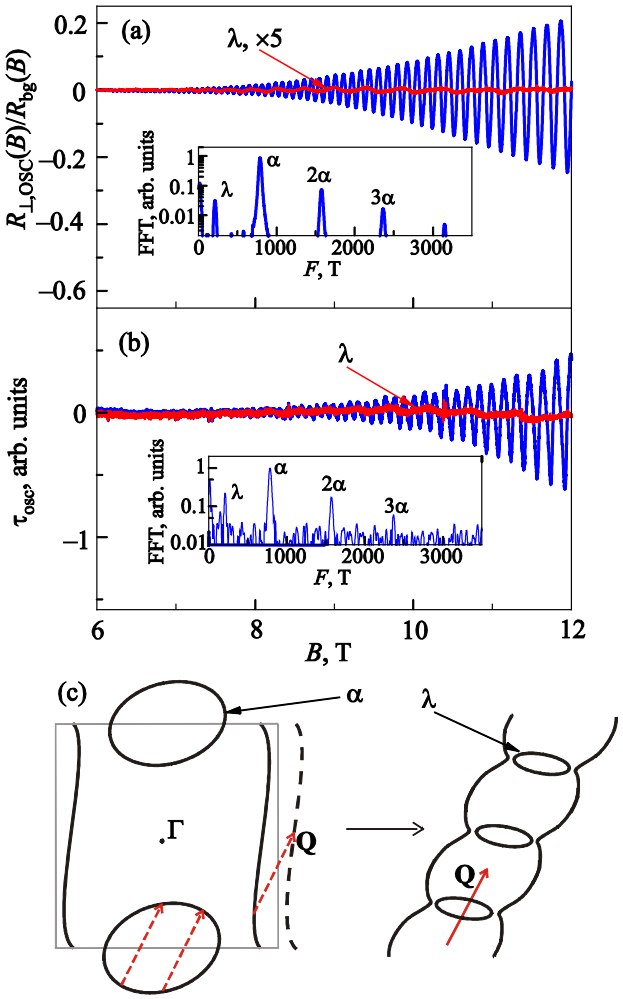

Fig. 2. (Color online) Oscillating components of the magnetoresistance (a) and magnetic torque (b) of the K-salt at $T = 0.45$ K, $\theta = 31.5°$. The red curves are obtained by filtering out the α-oscillations and demonstrate the behavior of the slow oscillations with frequency $F_\lambda = 210$ T. In (a) the λ-oscillations are magnified by a factor of 5, for a better visibility. The insets in (a) and (b) show the corresponding fast Fourier spectra. (c) Schematic 2D view of the Fermi surface reconstruction due to the CDW potential with the wave vector $\mathbf{Q}$. The original Fermi surface (left panel) consists of a pair of open sheets and a cylinder. The CDW, introducing a new periodicity with the wave vector $\mathbf{Q}$, opens a gap at the Fermi level in the whole open branch as well as in the q2D band at the states separated by $\mathbf{Q}$ (right panel).

open sheets of the original Fermi surface, sketched in the left panel of Fig. 2(c), also has an effect on the q2D band. It folds the cylindrical part of the Fermi surface, mixing the states with the wave vectors $\mathbf{k}$ and $\mathbf{k}+\mathbf{Q}$. This creates a new small cylinder and a pair of strongly corrugated sheets extending along $\mathbf{Q}$, as shown in the right panel of Fig. 2(c). The open sheets are responsible for the AMRO with sharp dips at the so-called Lebed magic angles [7,25,33]. The small cylindrical Fermi surface is manifested through the low-frequency MQO, F_λ. The α-oscillations come as a result of magnetic breakdown (MB).

The energy scale of the gap Δ separating the open and closed parts of the Fermi surface is of the order of the CDW potential, which can be assessed from the critical field of the low-temperature CDW_0–CDW_x phase transition, $\Delta \sim \pi\mu_B B_k$ [40–42]. For the K-salt, $B_k \approx 24$ T, yielding $\Delta \sim 4$ meV. Then, using the Blount criterion for MB [45], one can obtain an estimate of the breakdown field, $B_{MB} \sim \Delta^2 m_c/\hbar e E_F \sim 6$ T, where $E_F \sim 35$ meV and $m_c \approx 1.5 m_e$ are, respectively, the Fermi energy and effective cyclotron mass evaluated from the MQO data and e is the elementary charge.

At fields ~ 8 T, at which the MQO just become resolvable, the amplitudes of the λ- and α-oscillations coming from the classical and magnetic-breakdown orbits, respectively, are comparable. As the field increases further, the breakdown probability grows exponentially. This leads to a rapid enhancement of the α-oscillations by contrast to the almost constant amplitude of the λ-oscillations, c.f. blue and red lines in Fig. 2(a),(b). Above 17 T the relative contribution of the λ-frequency to the MQO spectrum becomes vanishingly small due to the strong magnetic breakdown. The latter is also reflected in the negative slope of the magnetoresistance, see Fig. 1, as well as in the behavior of the AMRO [46]. As the system enters the CDW_x state at B_k, the CDW gap is considerably reduced [41,42]. The probability of magnetic breakdown increases to almost unity; both the MQO and classical magnetoresistance are fully determined by the breakdown orbit α, as if the cylindrical Fermi surface were unreconstructed. In particular, this is a reason why the high-field CDW_x state was for some time confused with a reentrant normal state [47,48].

Besides the frequencies F_α and F_λ, their linear combinations have been observed in some experiments [25,26,46], which is consistent with the proposed model of the Fermi surface reconstruction. An additional frequency of 775 T has been reported once for the K-salt [46] that would be difficult to account for. However, to the best of our knowledge, it has not been reproduced by other authors. It should be noted that there is still no simple explanation of the anomalously strong second harmonic of F_α observed in the CDW_0 state at field orientations nearly normal to the layers. In spite of several attempts to explain them [49,50], this puzzle is still awaiting a convincing solution.

4. Phase inversion of the SdH oscillations

There is a notable difference in the behavior of the dHvA and SdH signals in Fig. 1. While the magnetization displays regular oscillations continuously growing with field, the SdH signal has a node-like feature at 26 T, i.e., shortly after entering the CDW_x state. The phase of the SdH oscillations inverts at the node. On the high-field side the positions of the resistance peaks coincide with the midpoints of the decaying half-periods of the magnetization oscillations corresponding to the integer filling factors (the chemical potential resides in the middle between the adjacent Landau levels). This is exactly what is expected of the interlayer magnetoresistance oscillations in the bulk q2D regime, when the Landau level (LL) spacing $\hbar\omega_c$ exceeds the interlayer bandwidth $4t_\perp$ [10,15,51,52]. At first glance, the inverted phase of the SdH oscillations below the node-like feature might be attributed to a dimensional crossover from the high-field q2D regime to a more conventional 3D one, where the resistance should peak at odd-half-integer filling [45,53]. This, however, is hardly the case: due to a very weak interlayer coupling, the dimensional crossover in the present materials takes place already at 1–2 T [14,19]. Therefore, the oscillation phase below the node should be considered as anomalous.

At ambient pressure, the phase inversion occurs only in the CDW_x state, above 24 T that makes it rather difficult to trace in steady magnetic fields. Therefore, we have performed magnetoresistance measurements under pressure which is known to shift the CDW phase boundaries to lower fields and temperatures [54]. The results of the experiment on the K-salt under a pressure of 1.8 kbar, in the field perpendicular to the layers are summarized in Fig. 3. In panel (a) the SdH oscillations, obtained by subtracting a low-order polynomial from the as-measured interlayer resistance, are plotted as a function of inverse field for different temperatures. The solid (dashed) grid lines are drawn through the maxima (minima) of the resistance at 4.2 K. The lower-temperature curves show an inversion of the oscillation phase within narrow field intervals marked by hatched boxes. Following the results of the ambient pressure experiment, we conclude that also under pressure the SdH phase is "correct" (resistance maxima at integer filling factors) at high fields and anomalous at lower fields.

Note that the field $B_{\rm pi}$, at which the phase inversion occurs, rapidly increases at lowering the temperature. This obviously is reflected in the temperature dependence of the oscillation amplitude, leading to drastic deviations from the conventional Lifshitz–Kosevich behavior [55,56]. Indeed, according to the data in Fig. 3(a), the T-dependence of the SdH amplitude measured at around 28 T ($1/B = 0.036$ T^{-1}) reaches its maximum at 2.6 K and nearly vanishes at 1.4 K; at fields 25–26 T the amplitude has a minimum near 2 K. Therefore, one has to be extremely careful when trying to analyze the T-dependence of the SdH amplitude in the present system in terms of the Lifshitz–Kosevich theory.

The temperature-dependent field $B_{\rm pi}$ is plotted in Fig. 3(b) (stars) on top of the phase diagram of the K-salt at 1.8 kbar (circles). For $T = 4.2$ K no phase inversion was detected down to 15 T, the lowest field at which the oscillations could still be resolved; therefore, the point at 4.2 K only indicates the upper limit for $B_{\rm pi}$. From this plot it becomes clear that the anomalous SdH phase exists only in the CDW state, at temperatures and fields sufficiently distant from the boundary to the normal state.

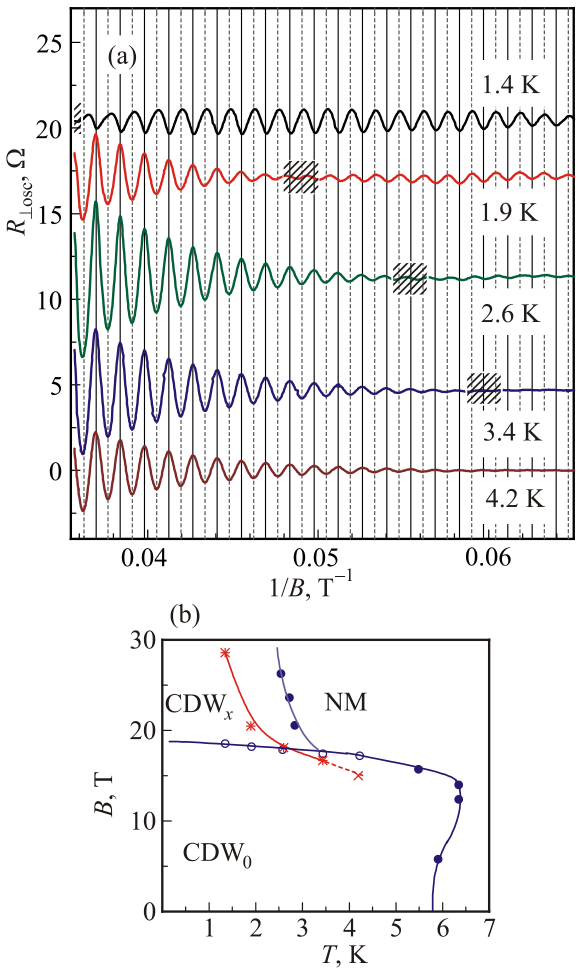

Fig. 3. (Color online) (a) Oscillations of the interlayer resistance of the K-salt under pressure P = 1.8 kbar plotted in the 1/B scale, for different temperatures. The vertical solid (dashed) grid lines correspond to the integer (odd half-integer) filling factors, see text. The hatched boxes indicate the regions where the oscillation phase changes by π. (b) The T – B phase diagram (filled and empty blue circles), taken from Ref. 54, and the phase inversion points (red stars) determined from the data in (a).

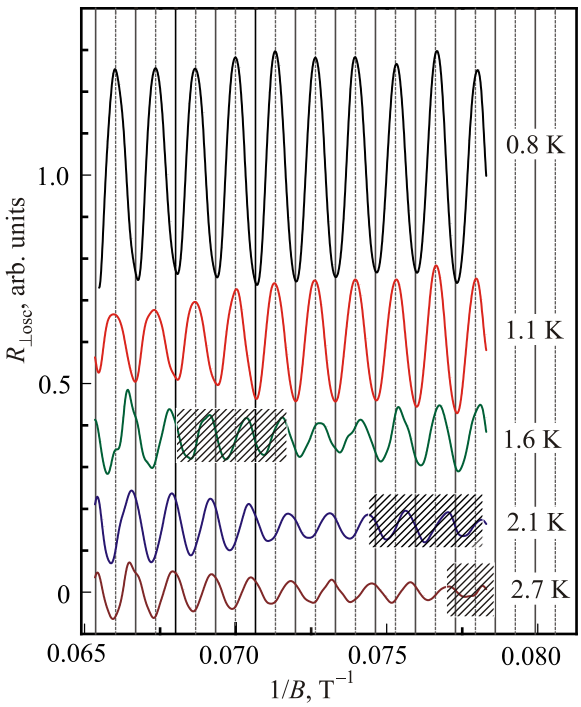

Fig. 4. (Color online) The same plot as in Fig. 3(a) but for the Tl-salt under pressure P = 2.6 kbar.

To verify that the anomalous SdH phase is a general property of the CDW state of α-(BEDT-TTF)$_2$MHg(SCN)$_4$ and not just a feature of the K-salt, we made similar measurements on the Tl-salt under a pressure of 2.6 kbar. Figure 4 shows the oscillating component of magnetoresistance in the inverse-field scale. While no perfect nodes are observed in this case, the oscillations clearly invert their phase upon changing field and temperature. Note that the data in Fig. 4 correspond to the field range below 15.5 T which is significantly below the CDW$_0$–CDW$_x$ transition. Thus, the phase inversion in the field sweeps occurs deep inside the CDW$_0$ phase for temperatures above 1.5 K.

The inversion of the SdH signal in the α-(BEDT-TTF)$_2$MHg(SCN)$_4$ compounds has already been reported by a number of authors [28,55–58]. Most of these experiments were focused on the high-field state, above the kink field B_k. Consequently, all the proposed explanations, involving various exotic phenomena such as bulk quantum Hall effect [56,59], Froehlich superconductivity [28], or an unconventional quantum liquid [32], associated the anomalous phase with the high-field CDW$_x$ or even normal state. They all implied a normal behavior to be restored at lower fields as the system enters the CDW$_0$ state and/or the oscillations become weak. This obviously contradicts the present results showing that the anomalous phase does exist in the CDW$_0$ state. Moreover, no re-entrance to the normal phase is observed at lowering the field as long as the oscillations can be resolved. Therefore, the mechanism responsible for the phase inversion should be based on a property common for the CDW$_0$ and CDW$_x$ states. A possible candidate is magnetic breakdown between the open and closed parts of the q2D Fermi surface. Below we propose a model, illustrating how magnetic breakdown may lead to the phase inversion of the SdH signal in a system with spatial fluctuations of the breakdown gap, and argue that it is qualitatively consistent with the present experiment.

5. Model of spatially inhomogeneous magnetic breakdown

The observed magnetoresistance is due to two subsets of electron orbits in the momentum space. The first one appears due to MB and corresponds to the closed electron trajectory along the α-pockets of the Fermi surface, see Fig. 2(c). This orbit is responsible for the quantum oscillations with the frequency F_α and would be the only one observed for the breakdown amplitude p = 1. The second

subset includes all other trajectories on the reconstructed Fermi surface: open trajectories on the strongly corrugated open sheets, closed orbits on the very small FS cylinders, yielding the MQO frequency F_λ, as well as a variety of other MB orbits, which do not contribute to the α-frequency of MQO. The main contribution to the electron density of states (DoS) of the second subset comes from the states on the open non-quantized orbits. Hereafter we refer to this second subset as to the open or q1D branch, whereas the first subset, producing the α-frequency, we call the q2D branch. At a finite MB amplitude both branches are present. To encircle the α-orbit, electrons must undergo four MB transitions, see Fig. 2(c). Therefore, the amplitude to complete the α-orbit is $p^4 R_D$ [60], where p is MB amplitude and R_D is the Dingle factor coming from the electron scattering on short-range defects [61]; in clean samples R_D is close to unity. Hence, in analogy to the case of MQO in the regime of a finite MB amplitude p [60], we may very roughly evaluate the density of q2D electron states as $\rho_{2D}(\varepsilon) \approx |p|^4 \rho(\varepsilon)$, and the density of the q1D states as $\rho_{1D}(\varepsilon) = (1-|p|^4)\rho(\varepsilon)$, where $\rho(\varepsilon)$ is the total DoS [62]. In our experiment the MB amplitude at $B = 20$ T is close to unity: $|p| = \exp(-B_{MB}/2B) \simeq 0.86$, using the given above estimate $B_{MB} \simeq 6$ T. However, the relative weight of the q1D states is still comparable to that of q2D states: $1-p^4 \approx 0.45$. The significant contribution from the q1D states is manifested, for instance, in the AMRO behavior.

The MB with a finite amplitude induces transitions between these two branches: from the q1D to the q2D branch with the amplitude p and probability $|p|^2$, and to the q1D branch with the amplitude $q = e^{i\varphi}\sqrt{1-|p|^2}$ and probability $1-|p|^2$. For an ideal crystal, the MB amplitude does not depend on coordinates. However, in various organic metals the CDW order parameter is subject to spatial fluctuations, as in the soliton phase of the CDW (see, e.g., Refs. 63 and 64 for review). These solitons locally reduce the CDW gap value Δ_{CDW}. Since the CDW gap defines the MB gap, namely, $B_{MB} \propto \Delta_{CDW}^2$, the MB amplitude p significantly increases in such soliton spots. For simplicity, consider the MB amplitude $p = p_0(B)$ everywhere except for certain "MB defect" spots, where $p = p_1 \approx 1$. This means that the defect spots scatter the electrons to the q2D states. The scattered electrons change their momentum in the direction perpendicular to the layers (z direction) because the MB defects are local, which leads to relaxation of the z-component of electron momentum as if due to impurities.

In spite of an obvious similarity between the MB-defect spots and randomly distributed impurities, there is an important difference between the two: the latter scatter electrons to any state with the same energy, and in the Born approximation the corresponding scattering rate is $1/\tau_i \propto \rho(\varepsilon)$, where the total DoS $\rho(\varepsilon)$ is the sum of the q1D and the q2D DoS: $\rho(\varepsilon) = \rho_{1D}(\varepsilon) + \rho_{2D}(\varepsilon)$. In our model, the MB defects scatter electrons only to the q2D branch, and their scattering rate is

$$1/\tau_{MB} \propto \rho_{2D}(E_F). \tag{1}$$

In the τ-approximation the interlayer conductivity

$$\sigma_{zz} = 2e^2\tau_{\text{tot}} \sum_{\mathbf{k},\alpha} v_{z\alpha}^2(\mathbf{k})\left(-n_F'\left[\varepsilon_\alpha(\mathbf{k})\right]\right), \tag{2}$$

where α labels the branch, the total scattering rate is given by the sum of the contributions from MB defects and from impurities:

$$1/\tau_{\text{tot}} = 1/\tau_{MB} + 1/\tau_i,$$

and $v_{z1D(2D)}$ is the z-component of the electron velocity on the q1D (q2D) part of the spectrum. The derivative of the Fermi distribution function is

$$n_F'(\varepsilon) = -1/\{4T\cosh^2[(\varepsilon - E_F)/2T]\} \to \delta(\varepsilon - E_F)$$

at $T \to 0$, and Eq. (2) simplifies to

$$\sigma_{zz} = 2e^2\tau_{\text{tot}}(E_F)\sum_\alpha \left\langle v_{z\alpha}^2 \right\rangle \rho_\alpha(E_F),$$

where $\langle ... \rangle$ denotes averaging over the states on the α-th sheet of the Fermi surface. In very clean samples, $1/\tau_{MB} \gg 1/\tau_i$, so that the main relaxation of electron momentum arises from the scattering off MB defects:

$$1/\tau_{\text{tot}} \approx 1/\tau_{MB}. \tag{3}$$

Incidentally, the increasing scattering rate in the MB regime may account for the unusually strong magnetoresistance of the present compounds at $B \sim 10$ T, see Fig. 1.

Combining Eqs. (1)–(3) we obtain

$$\sigma_{zz} \propto \frac{\left\langle v_{z1D}^2 \right\rangle \rho_{1D}(E_F) + \left\langle v_{z2D}^2 \right\rangle \rho_{2D}(E_F)}{\rho_{2D}(E_F)}. \tag{4}$$

Due to the Landau quantization, the q2D DoS $\rho_{2D}(E_F)$ is an oscillating function of $E_F/\hbar\omega_c$ around some constant value ρ_{2D0}. For the q1D branch, there is no LL quantization, and the q1D DoS does not oscillate: $\rho_{1D}(E_F) \approx \rho_{1D0}$.

The mean-square velocity on the q2D branch $\left\langle v_{z2D}^2 \right\rangle$ is also an oscillating function of $E_F/\hbar\omega_c$, but the amplitude and even the sign of its oscillations depends on the ratio of $t_\perp$, $\hbar\omega_c$ and $\hbar/\tau$. In 3D metals with $t_\perp \gg \hbar\omega_c$ the oscillations of $\left\langle v_{z2D}^2 \right\rangle$ are weak and in the opposite phase to the DoS oscillations, which determine the phase of SdH oscillations in 3D metals. In almost 2D metals with $t_\perp \ll \hbar\omega_c$ but for weak MQO, the oscillations of $\left\langle v_{z2D}^2 \right\rangle$ are still much weaker than the oscillations of $\rho_{2D}(E_F)$.

To show this, consider $\left\langle v_{z2D}^2 \right\rangle = I(E_F)/\rho_{2D}(E_F)$, where the quantum oscillations of $I(E_F) \equiv \sum_{FS} v_{z2D}^2$ are given by Eq. (3) of Ref. 65 and the oscillations of $\rho_{2D}(E_F) = 1/\tau_i(E_F)$ are given by the Eq. (2) of Ref. 65. At $t_\perp \ll \hbar\omega_c$, if we keep only the fundamental harmonic of MQO, this gives

$$\rho_{2D}(\varepsilon) \propto 1 - 2R_D \cos\left(2\pi\varepsilon/\hbar\omega_c\right), \qquad (5)$$

where R_D is the Dingle factor, and

$$I(\varepsilon) \propto 1 - 2R_D \cos\left(2\pi\varepsilon/\hbar\omega_c\right) \propto \rho_{2D}(\varepsilon),$$

i.e., $\left\langle v_{z2D}^2 \right\rangle = I(E_F)/\rho_{2D}(E_F) = \text{const}$ up to the terms of the order of R_D^2. Hence, for $R_D \ll 1$ at $t_\perp \ll \hbar\omega_c$,

$$\left\langle v_{z2D}^2 \right\rangle \approx \left\langle v_{z1D}^2 \right\rangle \approx 2t_\perp^2 d^2/\hbar^2. \qquad (6)$$

For strong MQO in almost 2D metals, i.e., when $R_D \approx 1$ and $t_\perp \ll \hbar\omega_c$, the oscillations of $\left\langle v_{z2D}^2 \right\rangle$ cannot be neglected and must be calculated beyond the τ-approximation [10,51,52]. In this limit the oscillations of $\left\langle v_{z2D}^2 \right\rangle$ are in phase with the oscillations of $\rho_{2D}(\varepsilon)$:

$$\left\langle v_{z2D}^2 \right\rangle(\varepsilon) \approx \left\langle v_{z1D}^2 \right\rangle \left[1 - 2\beta R_D \cos\left(2\pi\varepsilon/\hbar\omega_c\right)\right], \qquad (7)$$

where the effective parameter $\beta \lesssim 1$ depends on magnetic field.

Substituting Eqs. (5) and (7) to Eq. (4) we obtain

$$\sigma_{zz} \propto \text{const} + \left(\frac{\rho_{1D0}}{\rho_{2D0}} - \beta\right) 2R_D \cos\left(2\pi F/B\right). \qquad (8)$$

For comparison, in the case of impurity scattering only, i.e. without MB defects, in a quasi-2D limit we have [45]

$$\sigma_{zz} \propto 1 - 2R_D \cos\left(2\pi F/B\right). \qquad (9)$$

Hence, within the model above, the SdH oscillations change their sign when the ratio ρ_{1D0}/ρ_{2D0} crosses β. Thus, spatial fluctuations of magnetic breakdown may lead to a phase inversion of the SdH signal in a field sweep. Since the MB gap, determined by the CDW potential is small near the CDW – normal-metal boundary, the anomalous phase only occurs at certain temperatures well enough below the CDW transition. This explains the *T*-dependence of the phase inversion field. Finally, according to Fig. 3(b), the anomalous phase is apparently less stable in the CDW_x state, which has a much larger concentration of solitons. Within the proposed model, this is obviously related to the significant drop of the CDW gap upon entering this high-field state.

Acknowledgments

This work has been supported by the German Research Foundation grant KA 1652/4-1, by the Russian Foundation for Basic Research grants Nos. 12-02-00312 and 13-02-00178, and by SIMTECH Program grant 246937. The experiments in fields above 15 T were supported by the LNCMI-CNRS, member of the European Magnetic Field Laboratory (EMFL). The visit of P.D.G. to the LPT Toulouse was supported by l'Agence Nationale de la Recherche under the program ANR-11-IDEX-0002-02, reference ANR-10-LABX-0037-NEXT.

1. A.P. Cracknell and K.C. Wong, *The Fermi Surface*, Oxford University Press, London (1973).
2. L. Taillefer, *J. Phys.: Condens. Matter* **21**, 164212 (2009).
3. M.V. Kartsovnik, T. Helm, C. Putzke, F.W.-F.I. Sheikin, S. Lepault, C. Proust, D. Vignolles, N. Bittner, W. Biberacher, A. Erb, J. Wosnitza, and R. Gross, *New J. Phys.* **13**, 015001 (2011).
4. P. Walmsley, C. Putzke, L. Malone, I. Guillamon, D. Vignolles, C. Proust, S. Badoux, A. Coldea, M. Watson, S. Kasahara, Y. Mizukami, T. Shibauchi, Y. Matsuda, and A. Carrington, *Phys. Rev. Lett.* **110**, 257002 (2013).
5. D. Graf, R. Stillwell, T.P. Murphy, J.-H. Park, E.C. Palm, P. Schlottmann, R.D. McDonald, J.G. Analytis, I.R. Fisher, and S.W. Tozer, *Phys. Rev. B* **85**, 134503 (2012).
6. L. Taillefer, R. Newbury, G. Lonzarich, Z. Fisk, and J. Smith, *J. Magn. Magn. Mater.* **63–64**, 372 (1987).
7. M.V. Kartsovnik, *in: The Physics of Organic Superconductors and Conductors*, A.G. Lebed (ed.), Springer Verlag, Berlin Heidelberg (2008), p. 185.
8. M.V. Kartsovnik, *Chem. Rev.* **104**, 5737 (2004).
9. M.V. Kartsovnik and V.G. Peschansky, *Fiz. Nizk. Temp.* **31**, 249 (2005) [*Low Temp. Phys.* **31**, 185 (2005)].
10. P.D. Grigoriev, *Phys. Rev. B* **88**, 054415 (2013).
11. H. Mori, S. Tanaka, M. Oshima, G. Saito, T. Mori, Y. Maruyama, and H. Inokuchi, *Bull. Chem. Soc. Jpn.* **63**, 2183 (1990).
12. R. Rousseau, M.-L. Doublet, E. Canadell, R.P. Shibaeva, S.S. Khasanov, L.P. Rozenberg, N.D. Kushch, and E.B. Yagubskii, *J. Phys. I France* **6**, 1527 (1996).
13. N. Hanasaki, S. Kagoshima, N. Miura, and G. Saito, *Phys. Rev. B* **63**, 245116 (2001).
14. M.V. Kartsovnik, D. Andres, S.V. Simonov, W. Biberacher, I. Sheikin, N.D. Kushch, and H. Müller, *Phys. Rev. Lett.* **96**, 166601 (2006).
15. N. Harrison, R. Bogaerts, P.H.P. Reinders, J. Singleton, S.J. Blundell, and F. Herlach, *Phys. Rev. B* **54**, 9977 (1996).
16. V.N. Laukhin, A. Audouard, H. Rakoto, J.M. Broto, F. Goze, G. Coffe, L. Brossard, J.P. Redoules, M.V. Kartsovnik, N.D. Kushch, L.I. Buravov, A.G. Khomenko, E.B. Yagubskii, S. Askenazy, and P. Pari, *Physica B* **211**, 282 (1995).
17. M.M. Honold, N. Harrison, M.-S. Nam, J. Singleton, C.H. Mielke, M. Kurmoo, and P. Day, *Phys. Rev. B* **58**, 7560 (1998).

18. J. Wosnitza, S. Wanka, J. Hagel, R. Häussler, H. v. Löhneysen, J.A. Schlueter, U. Geiser, P.G. Nixon, R.W. Winter, and G.L. Gard, *Phys. Rev. B* **62**, R11973 (2000).
19. P.D. Grigoriev, M.V. Kartsovnik, and W. Biberacher, *Phys. Rev. B* **86**, 165125 (2012).
20. M.V. Kartsovnik, P.D. Grigoriev, W. Biberacher, and N.D. Kushch, *Phys. Rev. B* **79**, 165120 (2009).
21. P. Foury-Leylekian, J.-P. Pouget, Y.-J. Lee, R.M. Nieminen, P. Ordejón, and E. Canadell, *Phys. Rev. B* **82**, 134116 (2010).
22. T. Osada, R. Yagi, A. Kawasumi, S. Kagoshima, N. Miura, M. Oshima, and G. Saito, *Phys. Rev. B* **41**, 5428 (1990).
23. T. Sasaki, N. Toyota, M. Tokumoto, N. Kinoshita, and H. Anzai, *Solid State Commun*. **75**, 93 (1990).
24. M.V. Kartsovnik, A.E. Kovalev, V.N. Laukhin, and S.I. Pesotskii, *J. Phys. I France* **2**, 223 (1992).
25. M.V. Kartsovnik, A.E. Kovalev, and N.D. Kushch, *J. Phys. I France* **3**, 1187 (1993).
26. J. Caulfield, S.J. Blundell, M.S.L. du Croo de Jongh, P.T.J. Hendriks, J. Singleton, M. Doporto, F.L. Pratt, A. House, J.A.A.J. Perenboom, W. Hayes, M. Kurmoo, and P. Day, *Phys. Rev. B* **51**, 8325 (1995).
27. M.V. Kartsovnik, W. Biberacher, E. Steep, P. Christ, K. Andres, A.G.M. Jansen, and H. Müller, *Synth. Metals* **86**, 1933 (1997).
28. N. Harrison, L. Balicas, J.S. Brooks, and M. Tokumoto, *Phys. Rev. B* **62**, 14212 (2000).
29. D. Andres, M.V. Kartsovnik, P.D. Grigoriev, W. Biberacher, and H. Müller, *Phys. Rev. B* **68**, 201101(R) (2003).
30. D. Andres, M.V. Kartsovnik, W. Biberacher, K. Neumaier, I. Sheikin, H. Müller, and N.D. Kushch, *Fiz. Nizk. Temp*. **37**, 959 (2011) [*Low Temp. Phys*. **37**, 762 (2011)].
31. N. Harrison, E. Rzepniewski, J. Singleton, P.J. Gee, M.M. Honold, P. Day, and M. Kurmoo, *J. Phys.: Condens. Matter* **11**, 7227 (1999).
32. N. Harrison, J. Singleton, A. Bangura, A. Ardavan, P.A. Goddard, R.D. McDonald, and L.K. Montgomery, *Phys. Rev. B* **69**, 165103 (2004).
33. K. Uchida, R. Yamaguchi, T. Konoike, T. Osada, and W. Kang, *J. Phys. Soc. Jpn*. **82**, 043714 (2013).
34. D. Yoshioka, *J. Phys. Soc. Jpn*. **64**, 3168 (1995).
35. K. Maki, B. Dora, M. Kartsovnik, A. Virosztek, B. Korin-Hamzic, and M. Basletic, *Phys. Rev. Lett*. **90**, 256402 (2003).
36. H. Weiss, M.V. Kartsovnik, W. Biberacher, E. Balthes, A.G.M. Jansen, and N.D. Kushch, *Phys. Rev. B* **60**, R16259 (1999).
37. M.V. Kartsovnik, A.E. Kovalev, D.V. Mashovets, D.V. Smirnov, V.N. Laukhin, A. Gilewskii, and N.D. Kushch, *Physica B* **201**, 463 (1994).
38. P. Christ, W. Biberacher, M.V. Kartsovnik, E. Steep, E. Balthes, H. Weiss, and H. Müller, *JETP Lett*. **71**, 303 (2000).
39. C. Proust, A. Audouard, A. Kovalev, D. Vignolles, M. Kartsovnik, L. Brossard, and N. Kushch, *Phys. Rev. B* **62**, 2388 (2000).
40. A.I. Buzdin and V.V. Tugushev, *Zh. Eksp. Teor. Fiz*. **85**, 735 (1983) [*JETP* **85**, 428 (1983)].
41. D. Zanchi, A. Bjeliš, and G. Montambaux, *Phys. Rev. B* **53**, 1240 (1996).
42. P.D. Grigoriev and D.S. Lyubshin, *Phys. Rev. B* **72**, 195106 (2005).
43. R.W. Stark and R. Reifenberger, *J. Low Temp. Phys*. **26**, 763 (1977).
44. P.D. Grigoriev, *Phys. Rev. B* **67**, 144401 (2003).
45. D. Shoenberg, *Magnetic Oscillations in Metals*, Cambridge University Press, Cambridge (1984).
46. A. House, C.J. Hawoth, J.M. Caulfield, S. Blundell, M.M. Honold, J. Singleton, W. Hayes, S.M. Hayden, P. Meeson, M. Springford, M. Kurmoo, and P. Day, *J. Phys.: Condens. Matter* **8**, 10361 (1996).
47. T. Sasaki and N. Toyota, *Solid State Commun*. **82**, 447 (1992).
48. A. House, S. Blundell, M.M. Honold, J. Singleton, J.A. Perenboom, W. Hayes, M. Kurmoo, and P. Day, *J. Phys.: Condens. Matter* **8**, 8829 (1996).
49. T. Sasaki and T. Fukase, *Phys. Rev. B* **59**, 13872 (1999).
50. N. Harrison, N. Biskup, J.S. Brooks, L. Balicas, and M. Tokumoto, *Phys. Rev. B* **63**, 195102 (2001).
51. T. Champel and V.P. Mineev, *Phys. Rev. B* **66**, 195111 (2002).
52. P.D. Grigoriev, *Phys. Rev. B* **83**, 245129 (2011).
53. A.B. Pippard, *The Dynamics of Conduction Electrons*, Gordon and Breach, New York (1965).
54. D. Andres, M.V. Kartsovnik, W. Biberacher, H. Weiss, E. Balthes, H. Müller, and N. Kushch, *Phys. Rev. B* **64**, 161104(R) (2001).
55. S. Hill, P.S. Sandhu, J.S. Qualls, J.S. Brooks, M. Tokumoto, N. Kinoshita, T. Kinoshita, and Y. Tanaka, *Phys. Rev. B* **55**, R4891 (1997).
56. M.M. Honold, N. Harrison, M. Kartsovnik, H. Yaguchi, J. Singleton, C. Mielke, N. Kushch, M. Kurmoo, and P. Day, *Phys. Rev. B* **62**, 7908 (2000).
57. D. Andres, M.V. Kartsovnik, W. Biberacher, T. Togonidze, H. Weiss, E. Balthes, and N. Kushch, *Synth. Metals* **120**, 841 (2001).
58. S. Uji and J.S. Brooks, in *The Physics of Organic Superconductors and Conductors*, A.G. Lebed (ed.), Springer Verlag, Berlin–Heidelberg (2008), p. 89.
59. S. Hill, *Phys. Rev. B* **55**, 4931 (1997).
60. L.M. Falicov and H. Stachowiak, *Phys. Rev.* **147**, 505 (1966).
61. The total Dingle factor, measured from MQO, has contribution not only from the electron scattering on short-range defects but also from the long-range smooth potential, giving the local shift of the Fermi energy (see Refs. 19, 65 for details).
62. The MB amplitude is also energy-dependent: $p = p(\varepsilon)$. Below we take the values $\rho(\varepsilon)$, $\rho_{1D}(\varepsilon)$, $\rho_{2D}(\varepsilon)$ and $p(\varepsilon)$ at the Fermi level.
63. S. Brazovskii and N. Kirova, *Sov. Sci. Rev. A Phys*. **5**, 99 (1984).
64. W. Su and J.R. Schrieffer, in *Physics in One Dimension*, J. Bernascony and T. Schneider (eds.), Springer Verlag, Berlin–Heidelberg–New York (1981).
65. M.V. Kartsovnik, P.D. Grigoriev, W. Biberacher, N.D. Kushch, and P. Wyder, *Phys. Rev. Lett*. **89**, 126802 (2002).